Advanced Performance Materials 5, 193–200 (1998)

Mechanical Properties of LaRC™-IA and ULTEM® Melt-Extruded Fibers and Melt-Pressed Films

CATHARINE C. FAY, JEFFREY A. HINKLEY AND TERRY L. ST. CLAIR
NASA Langley Research Center, 6A West Taylor Street, Hampton, VA 23681

DENNIS C. WORKING
Mitsubishi Chemical America, 404 Volvo Pkwy, Chesapeake, VA 23320

Abstract. LaRC™-IA, the polyimide prepared with 3,4′-oxydianiline (3,4′-ODA) and oxydiphthalic anhydride (ODPA), is useful as a film, coating, adhesive, and composite matrix. The high temperature capability and fire-resistance of polyimides also makes them attractive candidates for textile fibers for a variety of uses in the automotive, chemical, and aerospace industries. This research describes for the first time the melt-spinning of phthalic anhydride endcapped LaRC™-IA and the effects of processing conditions on the mechanical properties of slightly-drawn fibers. Average draw ratios varied from 1 to 3.9. Tensile strengths ranged from 103 to 159 MPa; moduli ranged from 2.80 to 3.21 GPa; elongations at break ranged from 14 to 103%. For comparison, tensile properties of compression-molded films prepared at the same temperatures are also reported. Melt-extruded fibers and melt-pressed films of another thermoplastic, ULTEM®, were also fabricated. ULTEM® fibers exhibited tensile strengths ranging from 138 to 207 MPa for average draw ratios of 4.5 to 10.3. Moduli ranged from 2.70 to 3.22 GPa. Elongations at break ranged from 47 to 111%.

Keywords: melt-extrusion, polyimide fibers, tensile properties, LaRC™-IA, ULTEM®

Introduction

Aromatic polyimides are known for their outstanding thermal stability, excellent mechanical and electrical properties, and chemical resistance. These properties make them attractive for many applications. Much of the research to date has concentrated on polyimide films, coatings, resins and laminates. Another application of polyimides that has recently gained more attention is fibers.

Spinning processes are generally of three types. Dry-spinning involves passing a solution through a spinneret and blowing hot air on the filament to evaporate the solvent. In wet spinning, the solution is coagulated by passing it into a nonsolvent or reagent bath. Finally, melt-spun fibers are produced by extruding and drawing a polymer melt. In early polyimide fiber work by Irwin [1–2], various polypyromellitimide precursor fibers were dry-spun from poly(amic acid) (PAA) solutions. The PAA fibers were thermally converted to the polyimide under tension and further drawn at 550°C. Kaneda et al. [3] fabricated fibers derived from 3,3′,4,4′-biphenyltetracarboxylic dianhydride (BPDA) and various diamines. The PAAs were dissolved in *p*-chlorophenol and spun into a coagulating bath of ethanol. Sroog [4] summarizes reports of various polyimide fibers fabricated from PAA solutions and subsequently converted or drawn at temperatures ranging from 340 to 550°C. Solution

spinning and coagulation of fluorinated PAA solutions and polyimide resins were previously accomplished at NASA Langley Research Center [5].

Melt extrusion of thermoplastic polyimide powders would eliminate the need for solutions, coagulating baths, and additional processing to remove volatiles and to achieve thermal imidization. Melt-spun fibers have the properties to permit processing into useful articles using normal textile equipment [6].

Fiber composites utilizing high temperature resins such as poly(ether ether ketone) (PEEK), polyimide, and phenolic have exhibited fire-resistant properties [7–9]. Potential areas of application for such fibers might be fire-resistant fabrics for protective clothing, aircraft interiors or composite structures in the aircraft or automotive industries. Fibers that resist burning could be used in fabrics in heat resistant workwear (firefighters, professional race car drivers, pilots, etc). Polyimide fibers have potential for asbestos replacement. Fire safe fibers could be utilized in aircraft cabins for seating upholstery, tapestry, blankets, and carpeting applications. Fire safe fibers could be co-mingled with reinforcing media such as glass fiber, graphite fiber, and inert fillers to form, in-situ, melt-processable structures which would have utility in fire-resistant applications in the automotive and aerospace industries as thermal and electrical insulators and fire blocking layers. Additionally, polyimides are resistant to chemicals. Polyimide fibers could also be utilized in protective clothing for chemical workers or workers exposed to caustic environments.

Polyimides are resistant to moisture absorption. Polyimide fibers would have potential applications as marine cables, fishing nets, fishing line and fishing lures. Another application of polyimide fibers would be as rip stop materials for space applications. Large polymeric membranes used as thermal shields in space usually require rip stop as reinforcements. The rip stop material must be thermally and dimensionally stable. These fiber reinforcements must also be resistant to space environments such as ultraviolet radiation and atomic oxygen. Polyimide fibers would be useful in stitching applications, seat belts, slings, and rope.

LaRC^{TM}-IA is the reaction product of 3,4′-oxydianiline (3,4′-ODA) and 4,4′-oxydiphthalic anhydride (ODPA) which can be prepared in a variety of suitable solvents or via direct melt polymerization of these monomers. Endcapping with phthalic anhydride is used to control the number average molecular weight in the range of 10,000 to 20,000 g/mol. Previous studies on LaRC^{TM}-IA conducted at NASA have concentrated on end-uses such as films, coatings, adhesives, and composite matrices [10–17]. The present research deals with the production of melt-extruded LaRC^{TM}-IA fibers. The effects of processing conditions on the mechanical properties of slightly-drawn fibers and melt-pressed films are described. Melt-extruded fibers and melt-pressed films of another thermoplastic, ULTEM®, were also fabricated under the same conditions.

Experimental

Starting materials

LaRC^{TM}-IA (3% offset) powder was obtained from IMITEC, Inc. and dried in air at 192°C for 24 h prior to use. ULTEM® 1000 pellets were obtained from General Electric and dried in air at 192°C for 24 h prior to use.

Processing conditions

LaRC™-IA powder and ULTEM® pellets were melted and forced through an 8-filament spinneret using a single screw extruder operated at 10 rpm. Each capillary diameter was 0.343 mm. Fibers exiting the capillaries were drawn by gravity and cooled by ambient air. Three heights were utilized: 9.3 m, 5.3 m and 2.6 m. At each height fibers were extruded at three temperatures: 340, 350 and 360°C. Apparent draw ratios were calculated by: area of die/final area of fiber [18]. Die swell was not determined.

Melt-pressed films were fabricated in stainless steel molds using a bench top Carver hydraulic press. Films were held at 340, 350 or 360°C for 30 minutes with pressures ranging from 0.34 to 1.38 MPa.

Characterization

Glass transition temperatures (T_g) were determined by differential scanning calorimetry (DSC) using a Shimadzu DSC-50 Thermal Analyzer or a Seiko DSC 210 at a heating rate of 20°C/min. Dynamic thermogravimetric analyses (TGA) were obtained in flowing air (40 cm^3/min or 50 cm^3/min) at a heating rate of 2.5°C/min after an initial 30 min hold at 100°C using a Seiko Model TG/DTA 220 or Seiko TGA Model 5200. The temperature at which 5% weight loss occurred was reported.

A model 2000/2 table-top MTS Systems Corp. SINTECH load frame, equipped with Compaq Model 486 computer and HP graphics plotter, was used for measuring tensile properties. Fiber diameters were measured using a micrometer. A gage length of 7.6 cm and crosshead speed of 4.6 cm/min were used for measuring fiber tensile properties. Film thicknesses were measured using an electronic micrometer. A gage length of 5.1 cm and a crosshead speed of 0.51 cm/min were used for measuring film tensile properties. All mechanical tests were performed at room temperature.

X-ray diffraction was performed using a Philips APD 3600, XRG 3100 equipped with a flat sample holder and copper radiation source. The excitation energy settings (source energy) were 45 kV and 40 mA. Wide angle X-ray diffraction was determined using a graphite monochromator with a 2 second time increment every 0.02° (2θ). The angular range was 5–40° (2θ). Small angle X-ray diffraction was determined using a Kratky camera with an angular range of 0.5–5.0° (2θ).

Results and discussion

In conventional fiber spinning, the filament diameter is controlled by varying the extruder throughput and the takeup speed. In the present study, however, the primary variable was drawing tension. During steady-state spinning, the polymer exiting the spinneret presumably expanded somewhat initially due to die swell and then was drawn by the weight of the fiber below it until it solidified.

The instantaneous stretch rate is proportional to the drawing force and inversely proportional to the elongational viscosity. An average rate of stretching [19] can be defined as

$$\bar{\dot{\varepsilon}} = (V_L - V_0)/L \tag{1}$$

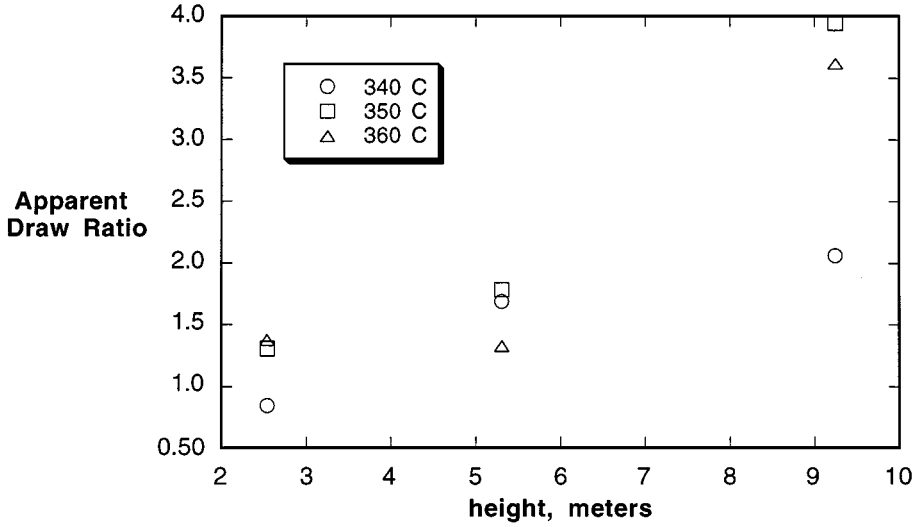

Figure 1. Apparent draw ratio of filaments as a function of extruder height and temperature.

where L is the distance traveled before solidification, V_0 is the initial velocity, and V_L is the velocity at the solidification point. If the height of the extruder is h, the drawing force is equal to the weight of the fiber, which is proportional to $A \cdot h$, where A is the fiber area $= \pi r^2 V_0 / V$. Substituting into Eq. (1) and rearranging we find that the draw ratio V_L / V_0 should be linear in the extruder height. As shown in figure 1, this is what was observed. The effect of extruder temperature is relatively small, and does not show up consistently in the data.

The full mathematical description of a cooling attenuating fiber is fairly complicated. In order to get a feel for the magnitudes of the relevant quantities, the following simplified case will be examined. We neglect axial conduction along the filament, and furthermore, assume the temperature is approximately constant through the diameter. Then the average fiber temperature can be obtained by solving the energy balance on a segment of the filament [20]:

$$q = GC_{\mathrm{p}}\Delta T \tag{2}$$

where q is the heat loss from the fiber surface, G is the mass flow rate, C_{p} is the polymer heat capacity, and ΔT is the axial temperature change.

The mass flow rate was not measured precisely, but was estimated to be about 1.6×10^{-5} kg/s per filament. This corresponds to an initial filament velocity of only 3 cm/s. The cooling was due to radiation, axial movement of the fiber, and natural convection. The appropriate free convection heat transfer coefficient for a slender vertical cylinder [21] is about 30 W/m^{2}K. Integrating Eq. (2), we find that the polymer reached its T_{g} about 40 cm below the orifice for any of the melt temperatures used. The average rate of extension $\bar{\dot{\varepsilon}}$ is then only on the order of 1 s^{-1}.

Table 1. Mechanical properties of LaRC™-IA fibers melt-extruded from a height of 9.3 m.

Processing temperature (°C)	Average fiber diameter (mm)	Mean modulus (GPa)	Mean tensile strength (MPa)	Mean elongation at break (%)
340	0.239	2.84	156	103
350	0.173	3.01	159	102
360	0.180	2.86	143	84

Table 2. Mechanical properties of LaRC™-IA fibers melt-extruded from a height of 5.3 m.

Processing temperature (°C)	Average fiber diameter (mm)	Mean modulus (GPa)	Mean tensile strength (MPa)	Mean elongation at break (%)
340	0.264	2.80	141	79
350	0.256	3.09	141	65
360	0.297	3.04	122	34

Table 3. Mechanical properties of LaRC™-IA fibers melt-extruded from a height of 2.6 m.

Processing temperature (°C)	Average fiber diameter (mm)	Mean modulus (GPa)	Mean tensile strength (MPa)	Mean elongation at break (%)
340	0.373	2.99	137	50
350	0.300	3.19	119	28
360	0.292	3.21	108	14

LaRC™-IA fibers melt-extruded at 340, 350 and 360°C and drawn by gravity from three heights exhibited draw ratios from 1 to 3.9. Tables 1–3 summarize the mechanical properties of LaRC™-IA fibers produced at various heights and temperatures. All fibers were amorphous by X-ray diffraction. There were no apparent systematic trends in the moduli with processing conditions, suggesting that the filaments were not highly oriented.

The degree of orientation in a melt-spun fiber is only weakly related to the draw ratio, but rather depends directly on the stress when the fiber reaches its final diameter [19]. In the present experiments, these stresses are equal to the weight of the filaments below the draw zone divided by the final diameter. To a first approximation, this quantity depends only on height, and amounts to only 0.1 MPa at the highest location. A faster takeup and lower drawing temperature should favor orientation.

It is customary, even with commodity textile fibers such as polyester, to produce a partially oriented yarn in the spinning operation, and then, in a separate operation, to draw it at moderate temperatures by a factor of perhaps 6 or so to induce crystallization.

Aromatic polyimides are known to be capable of crystallization. Furthermore, the high room temperature elongations in the tables suggest that further drawing and heat-setting should be feasible. In recent work performed under the direction of Prof. A. S. Abhiraman, crystallization of LaRC™-IA fibers was induced by drawing at 255°C, leading to modulus increases of a factor of four [22].

The slight decrease in elongation at the higher processing temperatures suggests that it may be advantageous to limit the extruder temperature when producing the initial amorphous fiber. T_g's of all samples were 229–230°C; however, any significant degree of oxidative degradation would have been expected to affect T_g. The temperature at which 5% weight loss occurred ranged from 506 to 519°C.

Glass transition temperatures for LaRC™-IA melt-pressed films were 226–228°C. The temperature at which 5% weight loss occurred ranged from 490 to 526°C. All films were amorphous by X-ray diffraction. The film data in Table 4 show that long (30 min) residence times at elevated temperatures lead to embrittlement.

Tables 5–7 summarize the mechanical properties of ULTEM® fibers extruded under the same conditions as the LaRC™-IA. Average apparent draw ratios are higher, varying from

Table 4. Mechanical properties of LaRC™-IA melt-pressed films.

Processing temperature (°C)	Mean modulus (GPa)	Mean tensile strength (MPa)	Elongation at break (%)
340	3.40	98.6	3.3
350	3.17	89.0	3.3
360	brittle	brittle	brittle

Table 5. Mechanical properties of ULTEM® fibers melt-extruded from a height of 9.3 m.

Processing temperature (°C)	Average fiber diameter (mm)	Mean modulus (GPa)	Mean tensile strength (MPa)	Mean elongation at break (%)
340	0.117	2.89	145	93
350	0.147	2.74	159	81
360	0.107	3.11	207	111

Table 6. Mechanical properties of ULTEM® fibers melt-extruded from a height of 5.3 m.

Processing temperature (°C)	Average fiber diameter (mm)	Mean modulus (GPa)	Mean tensile strength (MPa)	Mean elongation at break (%)
340	0.132	2.87	174	63
350	0.132	2.70	192	91
360	0.117	2.86	156	80

Table 7. Mechanical properties of ULTEM® fibers melt-extruded from a height of 2.6 m.

Processing temperature (°C)	Average fiber diameter (mm)	Mean modulus (GPa)	Mean tensile strength (MPa)	Mean elongation at break (%)
340	0.150	3.22	138	47
350	0.160	2.92	191	89
360	0.117	2.83	176	99

Table 8. Mechanical properties of ULTEM® melt-pressed films.

Processing temperature (°C)	Mean modulus (GPa)	Mean tensile strength (MPa)	Elongation at break (%)
340	2.70	108	7.3
350	2.59	98.6	5.6
360	2.44	88.9	8.5

4.5 to 10.3. This would be expected, since ULTEM® has a lower T_g, and presumably lower extensional viscosity at the same melt temperatures.

Tensile strengths generally increased with increasing processing temperature. Processing at 360°C generally resulted in the highest tensile strength, modulus and ultimate elongation among the temperatures used. Moduli did not vary in any systematic way with draw ratio in these amorphous fibers. It is not known whether ULTEM® can be induced to crystallize.

T_g's by DSC for the nine ULTEM® fiber samples varied from 216 to 220°C. The temperature at which 5% weight loss occurred ranged from 448 to 499°C. T_g's of melt-pressed films from ULTEM® 1000 pellets were 217–218°C. The temperature at which 5% weight loss occurred was 481°C for all ULTEM® film samples. Table 8 shows mechanical properties of ULTEM® melt-pressed films. Processing at 340°C resulted in the highest tensile strength and modulus. As with LaRC™-IA, tensile strengths and moduli decreased with increasing molding temperature. All film samples were amorphous by X-ray diffraction.

Conclusions

There is a need for fire-safe materials which exhibit better strength and serviceability, are lighter and can be installed in aircraft at lower costs. Fire-safe fibers are needed for seating upholstery, tapestry, blankets and carpeting. Drawn polyimide fibers exhibiting high strength and crystalline characteristics should have fire-resistant properties useful in next-generation cabin material applications. While the processing conditions and draw ratios were not optimized in this study, it was demonstrated that fully imidized LaRC™-IA and ULTEM® could be successfully melt-spun and drawn.

LaRC™-IA fibers melt-extruded at 340, 350 and 360°C and drawn by gravity from three heights exhibited draw ratios from 1 to 3.9. The highest tensile strengths and elongations

were obtained from the most highly-drawn fibers, although all the fibers produced in this study are thought to be suitable for secondary drawing to induce more orientation and crystallinity. Processing at 340 and 350°C resulted in better overall fiber mechanical properties than processing at 360°C.

Modulus, tensile strength and elongation at break of LaRC™-IA melt-pressed films likewise decreased with increasing processing temperatures. Tensile strengths of LaRC™-IA fibers were as much as 64% higher than tensile strengths of melt-pressed films.

ULTEM® 1000 pellets were melt-extruded under the same conditions as LaRC™-IA to give amorphous ULTEM® fibers. Average draw ratios ranged from 4.5 to 10.3. Moduli of fibers did not vary significantly. Higher fiber tensile strengths were achieved at processing temperatures of 340 and 350°C. Moduli of fibers were approximately 20% higher than moduli of melt-pressed ULTEM® films. Tensile strengths and moduli of melt-pressed films decreased with increasing processing temperature. ULTEM® fibers exhibited tensile strengths 55–90% higher than those of melt-pressed films. Elongations at break of ULTEM® fibers were also significantly higher.

References

1. R.S. Irwin, US Patent 3,415,782, E. I. DUPont & Co. (1968).
2. R.S. Irwin, US Patent 4,640,972, E. I. DUPont & Co. (1987).
3. T. Kaneda et al., J. Appl. Polym. Sci. **32**, 3133 (1986).
4. C.E. Sroog, Progr. Polym. Sci. **16**, 561 (1991).
5. W.E. Dorogy, Jr. and A.K. St. Clair, J. Appl. Polym. Sci. **49**, 501 (1993).
6. *Engineered Materials Handbook, Engineering Plastics* (ASM International, Metals Park, OH, 1988), vol. 2, pp. 378–388.
7. R.E. Lyon, Advanced fire-safe aircraft materials program, Final Report, January 1996, Office of Aviation Research DOT/FAA/AR-95/98.
8. U. Sorathia, T. Dapp, and J. Kerr, Fire and Materials **16**, 119 (1992).
9. R.G. Diehl, *Proceedings of the International Conference for the Promotion of Advanced Fire Resistant Aircraft Materials*, Atlantic City, NJ, 1993, pp. 93.
10. D.J. Progar and T.L. St. Clair, Journal of Adhesion Science and Technology **4**(7), 527 (1990); US Patent 5 147 966, NASA Langley Research Center (Sept. 1992).
11. C.I. Croall and T.L. St. Clair, Journal of Plastic Film and Sheeting **8**, 172 (1992).
12. C.C. Fay and A.K. St. Clair, Polymer Preprints **37**(1), 817 (1996).
13. T.H. Hou, N.J. Johnston, and T.L. St. Clair, High Performance Polymers **7**, 105 (1995).
14. P.R. McDaniel and T.L. St. Clair, Materials Research Society **405**, 535 (1995).
15. P.R. McDaniel and T.L. St. Clair, *Science and Technology of Atomically Engineered Materials*, edited by P. Jena, S.N. Khanna, and B.K. Rao (World Scientific, 1996), pp. 547.
16. A.C. Chang and T.L. St. Clair, US Patent 5,464,928, NASA Langley Research Center (1995).
17. T.L. St. Clair and A.C. Chang, NASA Tech Brief, May 1995.
18. *Extrusion and Other Plastics Operations*, edited by N.M. Bikales (Wiley-Interscience, New York, 1971), p. 35.
19. A.S. Abhiraman and G.E. Hagler, J. Appl. Polym. Sci. **33**, 809 (1987).
20. L.C.T. Lin and J. Hauenstein, J. Appl. Polym. Sci. **18**, 3509 (1974).
21. S.M. Yang, Heat transfer science and technology, *Proceedings of the International Symposium*, Beijing (Hemisphere Publ., Washington, DC, 1987), pp. 153–159.
22. K. Dorsey, Formation, morphology, and properties of oriented LaRC-IA filaments, Masters thesis, Department of Chemical Engineering, Georgia Institute of Technology, 1997.